Supporting Information

Rajon and Masel 10.1073/pnas.1012918108

SI Methods

The effects of mutations on α_{ik} or β_{ik} were sampled from normal distributions whose means depended on the value of α_{ik} or β_{ik}. Let $X(t)$ be a random variable corresponding to α_{ik} or β_{ik} at time t. Mutations are biased toward returning $X(t)$ toward 0, as shown in Eq. **S1**:

$$X(t+1) = X(t) + \text{norm}\left(\frac{-X(t)}{a}, \frac{\sigma}{K}\right) = \frac{a-1}{a}X_t + \text{norm}\left(0, \frac{\sigma}{K}\right). \quad [S1]$$

The expected value of the stationary distribution is obviously 0. The variance of X_{t+1} equals

$$V(X_{t+1}) = \left(\frac{a-1}{a}\right)^2 V(X_t) + \left(\frac{\sigma}{K}\right)^2. \quad [S2]$$

This recurrence equation can be solved by setting $V(X_{t+1}) = V(X_t) = V(X)$:

$$V(X) = \left(\frac{a-1}{a}\right)^2 V(X) + \left(\frac{\sigma}{K}\right)^2 = \frac{(\sigma/K)^2}{1-((a-1)/a)^2}. \quad [S3]$$

This value gives the expected variance of the distribution of the values of α_{ik} or β_{ik} at equilibrium without selection. The initial values (at the beginning of a simulation and after an assimilation event) of β_{ik} were sampled in a normal distribution with mean 0 and variance $V(X)$. The effects of mutations on α_{ik} and β_{ik} were sampled according to Eq. **S1**.

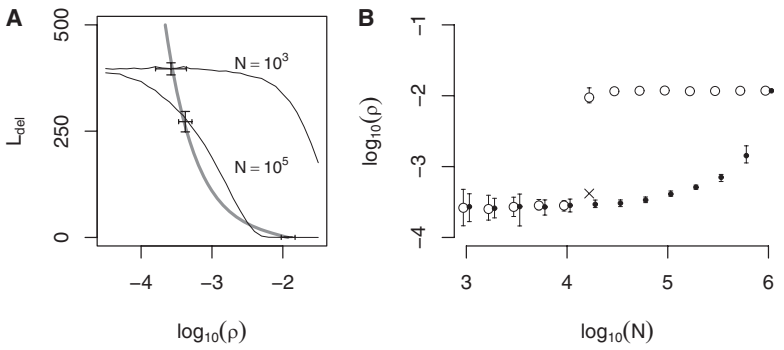

Fig. S1. (*A* and *B*) Evolutionary dynamics of the read-through error rate ρ under the additive fitness scenario. Results are very similar to those of the multiplicative scenario shown in Fig. 1 *A* and *B*. The error bars in *B* represent the 5% and 95% quantiles of the distributions of ρ in replicate populations. When $\log_{10}(N) = 4.25$, one replicate population with a high initial value of ρ (represented by a cross in *A*) reached the low-ρ attractor, which indicates an instability of the high-ρ attractor at this population size. Parameter values: $s = 14$, $p_{del} = 0.4$, $p_{-del} = 0.1$, $L_{tot} = 500$, $\delta = 10^{-2.5}$, and $\mu = 10^{-8}$.

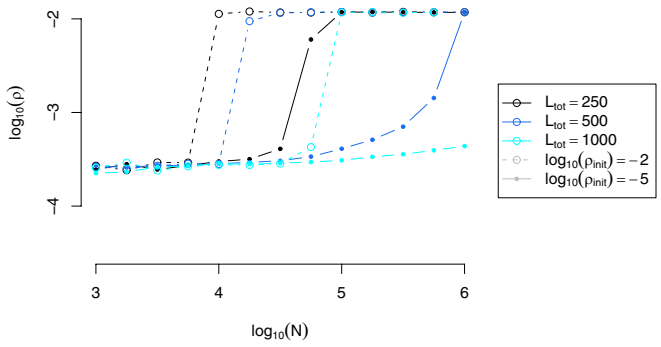

Fig. S2. The range of population sizes (N) for which the predicted rate of read-through errors (ρ) is bistable increases with the total number of loci, L_{tot}. In this regard, the results presented here (additive fitness scenario) are very similar to those obtained with the multiplicative fitness scenario (Fig. 1 and Fig. S1). However, the ratio of ρ between the two stable attractors does not change with L_{tot} in this scenario, whereas it increases in the case of multiplicative fitness effects (Fig. S4). Parameter values: $p_{del} = 0.4$, $p_{-del} = 0.1$, $\delta = 10^{-2.5}$, $\mu = 10^{-8}$, and $s = 14$.

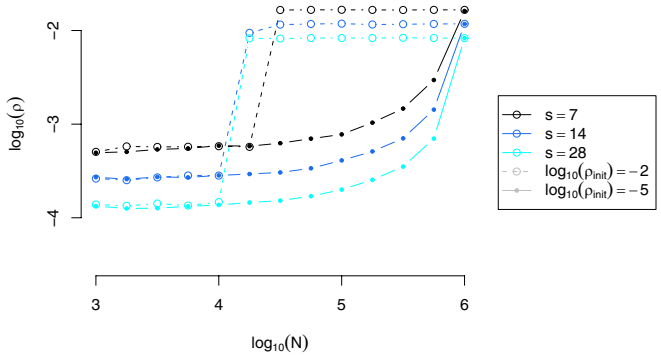

Fig. S3. The range of population sizes (N) for which the predicted rate of read-through errors (ρ) is bistable increases with s (the toxicity of deleterious products), due to a decrease in the lower bound of this range. The ratio of ρ between the two attractors increases with s. These results (additive fitness scenario) are very similar to those obtained in the multiplicative fitness scenario (Fig. S5), except that the range of N where ρ is bistable is slightly narrower in the latter case. Parameter values: $p_{del} = 0.4$, $p_{-del} = 0.1$, $L_{tot} = 500$, $\delta = 10^{-2.5}$, and $\mu = 10^{-8}$.

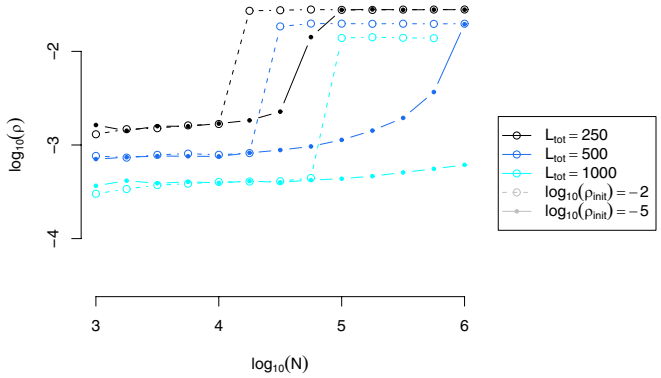

Fig. S4. The range of population sizes (N) for which the predicted rate of read-through errors (ρ) is bistable increases with the total number of loci, L_{tot}, as does the ratio of ρ between the two stable attractors. Parameter values: $p_{del} = 0.4$, $p_{-del} = 0.1$, $\delta = 10^{-2.5}$, $\mu = 10^{-8}$, and $\gamma = 0.01$ (multiplicative scenario).

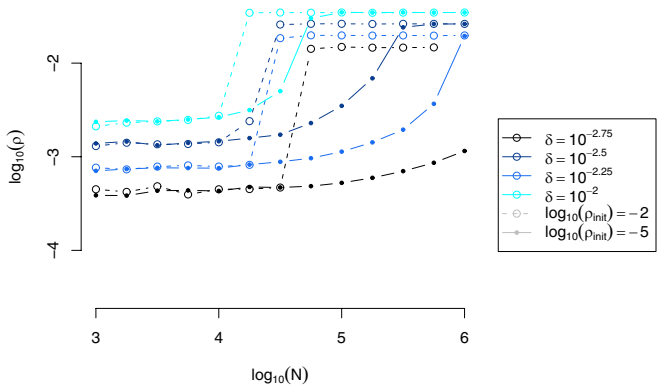

Fig. S5. The range of population sizes (N) for which the predicted rate of read-through errors (ρ) is bistable decreases when δ (the relative contribution of stop codon reading to the total amount of time needed for protein synthesis) increases, as does the ratio of ρ between the two stable attractors. Parameter values: $p_{del} = 0.4$, $p_{-del} = 0.1$, $L_{tot} = 500$, $\mu = 10^{-8}$, and $\gamma = 0.01$ (multiplicative scenario).

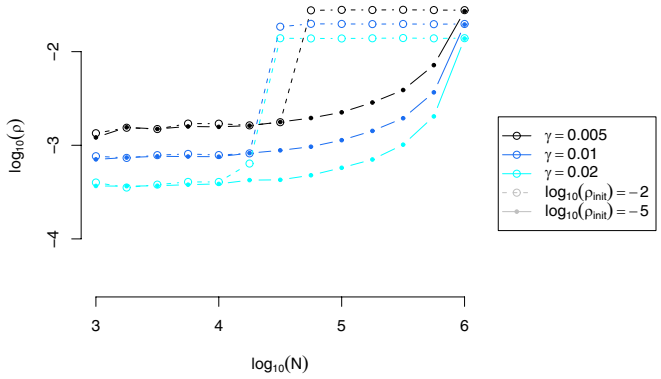

Fig. S6. The range of population sizes (N) for which the predicted rate of read-through errors (ρ) is bistable increases with γ, due to a decrease in the lower bound of this range. γ represents the curvature of the dose–response curve for gene dosage: Lower values of γ mean that partial loss of function has smaller fitness effects. The ratio of ρ between the two attractors also increases with γ. Parameter values: $p_{del} = 0.4$, $p_{-del} = 0.1$, $L_{tot} = 500$, $\delta = 10^{-2.5}$, and $\mu = 10^{-8}$.

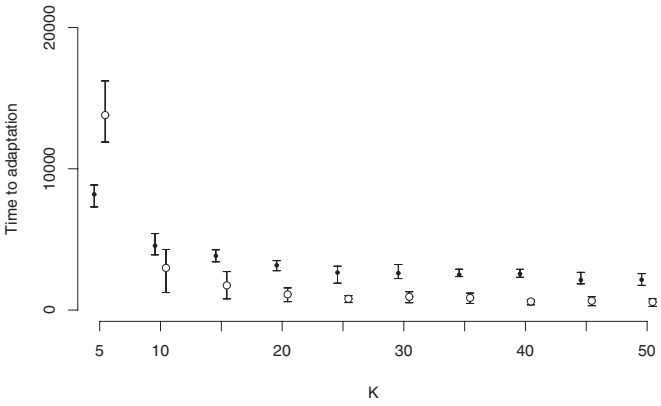

Fig. S7. Evolvability as a function of the number of loci coding for a trait when per locus mutational effects do not depend on K. Here, the SD of mutation effects equals 0.5 / 20 = 0.025. The numbers of adaptive mutations and assimilation events both increase with K. This dependence explains why the time to adaptation decreases with K, in contrast to Fig. 2*B*. As in Fig. 2*B*, the time to adaptation is always lower for the high-ρ attractor, except when $K = 5$ where the opposite result is found. This counterintuitive result for $K = 5$ is a consequence of hitchhiking. In our asexual populations, cryptic sequences hitchhike with adaptive fixations. In low-ρ populations in mutational equilibrium, positive and negative hitchhiking events cancel out. High-ρ populations with benign cryptic sequences have more to lose. These mildly deleterious effects of hitchhiking slow adaptation (1). This retardation happens for all values of K but for $K > 5$ this effect is swamped by the advantages of genetic assimilation. The error bars represent the first and third quartiles of the distribution of the time to adaptation, calculated over 20 simulations. The method for calculating the time to adaptation and the parameter values are the same as in Fig. 2 in the main text.

1. Desai M, Fisher DS (2007) Beneficial mutation–selection balance and the effect of linkage on positive selection. *Genetics* 176:1759–1798.

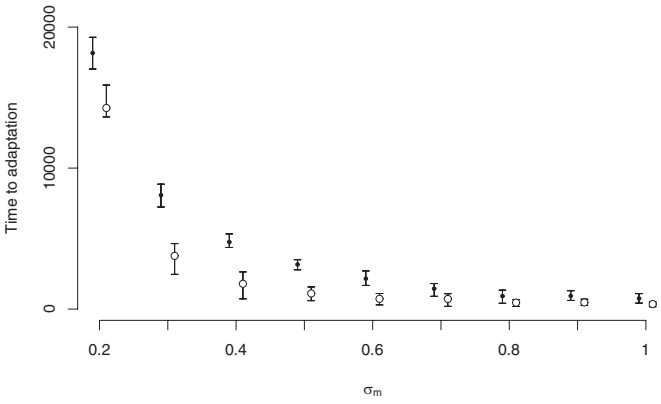

Fig. S8. The time to adaptation decreases with the SD of the effect of mutations, σ_m, and is consistently lower for the high-ρ attractor. The error bars represent the first and third quartiles in the distribution of the time to adaptation, calculated from 20 simulations for each set of parameter values. The two attractors are those shown in Fig. 1 *A* and *B* for $N = 10^5$. Parameter values: $N = 10^5$, $a = 750$; other values are the same as in Fig. 1 *A* and *B*.

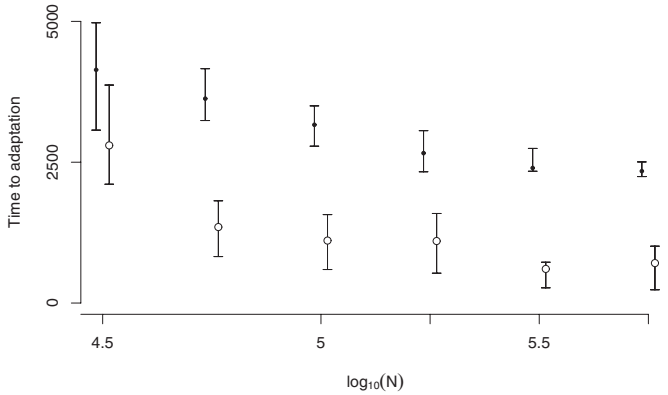

Fig. S9. The time to adaptation decreases as the population size N increases (within the range of values with a bistable outcome, Fig. 1) and is consistently lower for the high-ρ attractor (open circles). The error bars represent the first and third quartiles of the distribution of the time to adaptation, calculated over 20 simulations. The method for calculating the time to adaptation and the parameters values are the same as in Fig. 2, with $K = 20$, $\sigma_m = 0.5$, and $a = 750$.

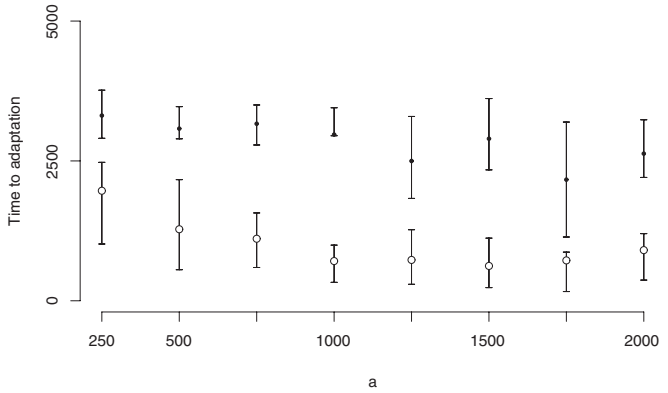

Fig. S10. The time to adaptation decreases with a (a limit to the variability of x) when ρ is high and is consistently lower for the high-ρ attractor. The error bars represent the first and third quartiles in the distribution of the time to adaptation, calculated from 20 simulations for each set of parameter values. The two attractors are those shown in Fig. 1 *A* and *B* for $N = 10^5$. Parameter values: $N = 10^5$, $\sigma_m = 0.5$; other values are the same as in Fig. 1 *A* and *B*.

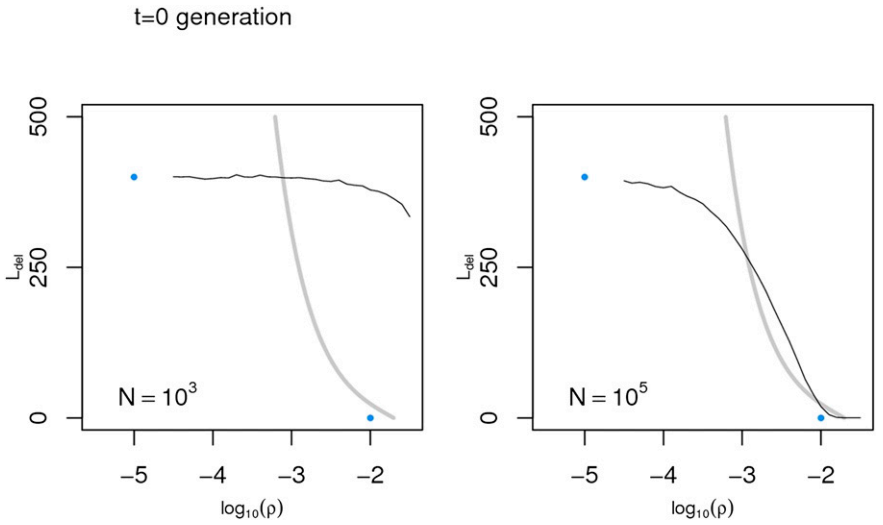

Movie S1. Coevolutionary dynamics of ρ and L_{del}. The coevolutionary dynamics are those whose endpoints are presented in Fig. 1*A* (see legend for parameter values) when $N = 10^3$ (*Left*) and $N = 10^5$ (*Right*). Each point in the video represents the population means of ρ and L_{del} in one of 40 replicate runs at a given time.

Movie S1